Electroexcitation of $M1$ and $M2$ resonances in spherical nuclei

A. I. Vdovin, V. Yu. Ponomarev, and V. M. Shilov

Joint Institute for Nuclear Research
(Submitted 31 December 1980)
Yad. Fiz. **34**, 1009–1019 (October 1981)

Current transition densities have been calculated for one-phonon 1^+ and 2^- states of spherical nuclei, using the quasiparticle-phonon nuclear model. It was found that the current transition densities of the 1^+ states are of surface type, and those of the 2^- states are of volume type. DWBA calculations of slow-electron large-angle-scattering differential cross sections using these current transition densities show that the electroexcitation probability for the 1^+ levels decreases sharply as compared with that for the 2^- levels as the momentum transfer and the target-nucleus mass number increase. This may account for the lack of success in searches for $M1$ resonances in intermediate and heavy nuclei.

PACS numbers: 24.30.Cz, 25.30.Cg

1. INTRODUCTION

Most of the experimental data on giant resonances, which have been intensively studied in recent years, have been obtained from electron inelastic scattering. It is sufficient to recall the studies of Pitthan and Walcher[1] and Fukuda and Torizuka,[2] in which the first of the "new" resonances—the isoscalar $E2$ resonance—was discovered, and the experiments of Lindgren *et al.*[3] and Richter *et al.*,[4] in which the $M2$ resonance was discovered.

The advantages of e, e' scattering in nuclear structure studies are generally known. Nevertheless, theoretical studies of giant resonances, as a rule, involve probabilities for electromagnetic transitions from the nuclear ground state to the resonance states. Still, the experimental $B(E\lambda)$ and $B(M\lambda)$ values with which the calculations are compared are obtained by processing e, e'-scattering data, frequently with the aid of rather primitive nuclear-structure models. It is doubtless more natural and informative to calculate the electron inelastic scattering cross section directly, using sufficiently sophisticated nuclear models. A number of such studies have already been carried through. In processing data from e, e' experiments, the Darmstadt group uses wave functions for nuclear excitations calculated within the framework of the semimicroscopic MSI model,[5] and form factors for electron scattering with excitation of giant resonances have been investigated by Goncharova *et al.*[6] Cross sections for electron and α-particle inelastic scattering with excitation of giant resonances in spherical nuclei have recently been calculated within the framework of the theory of finite Fermi systems.[7]

In the present work we use the distorted wave Born approximation (DWBA) to treat the inelastic scattering of electrons with excitation of $M1$ and $M2$ resonances in spherical nuclei. The wave functions for the excited states of the even-even nuclei are calculated in the random phase approximation (RPA), the effective forces between the nuclear nucleons being represented as a sum of ordinary pairing forces and separable spin-multipole forces.[8] Using separable effective forces with an $r_1^\lambda r_2^\lambda$ radial dependence, the authors of Ref. 9 obtained good agreement with the experimental data on the form factors for e, e' scattering with excitation of low-lying vibrational levels and $E1$ and $E2$ resonances in spherical and deformed nuclei. This allows one to hope that useful and reliable information may also be obtained for excitations of anomalous parity.

2. BASIC FORMULAS AND CALCULATION TECHNIQUES

The differential scattering cross sections were calculated in the framework of the DWBA with allowance for energy loss by the electron in the exit channel incident to excitation of the target nucleus.[10] If the nucleus, initially in the ground state Ψ_0, is excited to a state Ψ_f of anomalous parity as a result of interaction with the electron, then all the information on the structure of the state Ψ_f necessary to calculate the cross section for the process is contained in the current transition densities (CTD) $\mathbf{j}(\mathbf{r})$, which are defined as follows:

$$\mathbf{j}(\mathbf{r})=\mathbf{j}^c(\mathbf{r})+\mathbf{j}^m(\mathbf{r}), \tag{1}$$

$$\mathbf{j}^c(\mathbf{r})=-i\mu_N\sum_k \delta(\mathbf{r}-\mathbf{r}_k)g_l^k\{\Psi_f^*\nabla_k\Psi_0-\Psi_0\nabla_k\Psi_f^*\}, \tag{2}$$

$$\mathbf{j}^m(\mathbf{r})=\mu_N\sum_k \delta(\mathbf{r}-\mathbf{r}_k)g_s^k\nabla_k\{\Psi_f^*\mathbf{s}_k\Psi_0\}. \tag{3}$$

The summations in formulas (2) and (3) are taken over all the nuclear nucleons. Formula (1) should contain not only the convection current $\mathbf{j}^c(\mathbf{r})$ and the magnetic current $\mathbf{j}^m(\mathbf{r})$, but also another term, the so-called exchange current. We did not take the contribution from this term in the CTD into account directly, but our use of the renormalized nucleon gyromagnetic factors, rather than their free values, may to some extent be regarded as taking its effect into account effectively.

The wave functions for the initial and final states of the nucleus were calculated in the RPA. In this approximation the excited states of even-even nuclei are represented as superpositions of particle-hole configurations (or two-quasiparticle configurations if the pairing forces are taken into account). In the second-

 0038-5506/81/100561-06$02.20

quantization formalism, the one-phonon wave function is written as

$$\Psi_f = Q^+_{\lambda\mu i}\Psi_0 = \frac{1}{2}\sum_{jj'}\{\psi^{\lambda i}_{jj'}[\alpha^+_{jm}\alpha^+_{j'm'}]_{\lambda\mu} - (-1)^{\lambda-\mu}\varphi^{\lambda i}_{jj'}[\alpha_{j'm'}\alpha_{jm}]_{\lambda-\mu}\}\Psi_0, \quad (4)$$

where the operators α^+_{jm} and α_{jm} respectively create and destroy a quasiparticle on the average-field state with the quantum numbers $nljm$, and Ψ_0 is the wave function for the ground state of the even-even nucleus, which also represents the phonon vacuum ($Q_{\lambda\mu i}\Psi_0 = 0$) and in our case is the wave function for the initial state of the nucleus.

Since we are going to discuss the excitation of states having a definite multipolarity, it is useful to introduce the partial CTD $\rho^{c;m}_{\lambda i}(r)$, which are related as follows to the $\mathbf{j}^{c,m}(\mathbf{r})$:

$$\mathbf{j}^{c,m}(\mathbf{r}) = ec\sum_{\lambda i\mu}(-i)^l\hat{J}_f(-1)^{M_f-\lambda}\begin{pmatrix}0 & \lambda & J_f\\ 0 & \mu & -M_f\end{pmatrix}\rho^{c,m}_{\lambda i}(r)\mathbf{Y}^{\mu}_{\lambda l}(\Omega). \quad (5)$$

Magnetic excitations of multipolarity λ are determined by the functions $\rho^{c;m}_{\lambda\lambda}(r)$, whose form in the RPA for the initial- and final-state wave functions Ψ_0 and Ψ_f [Eq. (4)] are obtained by fairly simple manipulations that are described in detail in Ref. 11:

$$\rho^c_{\lambda\lambda}(r) = \mu_N\sum_{a\geqslant b} i^{l_b+\lambda+1-l_a}(-1)^{j_b+l_b+1/2}\hat{j}_a\hat{j}_b\hat{\lambda}\hat{\lambda}\sqrt{\frac{(2l_b-1)\overline{l_b}}{\pi}}$$
$$\times g_l^{n(p)}\begin{pmatrix}l_a & \lambda & l_b-1\\ 0 & 0 & 0\end{pmatrix}\begin{Bmatrix}l_a & l_b & \lambda\\ j_b & j_a & 1/2\end{Bmatrix}\begin{Bmatrix}l_b & 1 & l_b-1\\ \lambda & l_a & \lambda\end{Bmatrix}$$
$$\times\frac{u^{(-)}_{j_aj_b}}{1+\delta_{ab}}(\psi^{\lambda i}_{j_aj_b} - \varphi^{\lambda i}_{j_aj_b})\frac{2l_b+1}{r}u^*_a(r)u_b(r), \quad (6)$$

$$\rho^m_{\lambda\lambda}(r) = \mu_N\sum_{a\geqslant b} i^{l_b+1+\lambda-l_a}(-1)^{j_b+\lambda+1/2}\frac{\hat{j}_a\hat{j}_b}{4\sqrt{\pi}\lambda(\lambda+1)}g_s^{n(p)}\begin{pmatrix}j_a & j_b & \lambda\\ 1/2 & -1/2 & 0\end{pmatrix}$$
$$\times\frac{u^{(-)}_{j_aj_b}}{1+\delta_{ab}}(\psi^{\lambda i}_{j_aj_b} - \varphi^{\lambda i}_{j_aj_b})\left[\frac{\lambda(\lambda+1)'}{r} + (L_a+L_b)\left(\frac{d}{dr}+\frac{1}{r}\right)\right]u^*_a(r)u_b(r), \quad (7)$$

$$L_a = (l_a - j_a)(2j_a+1), \quad \hat{\lambda} = \sqrt{2\lambda+1}.$$

The summations in Eqs. (6) and (7) are taken separately over the neutron and proton single-particle states. The notation $a \geqslant b$ means that the states $|n_al_aj_a\rangle$ and $|n_bl_bj_b\rangle$ do not occur together twice in the sum. The coefficients $u^{(-)}_{j_aj_b} = u_{j_a}v_{j_b} - u_{j_b}v_{j_a}$ are combinations of the coefficients u and v in the Bogolyubov transformation.

The single-particle radial wave functions $u_a(r)$ (and their derivatives) were determined by numerical solution of the Schrödinger equation with a Woods-Saxon potential. For this calculation we used the REDMEL program, which yields a numerical solution of the Schrödinger equation for the spherically symmetric potential of finite depth proposed in Refs. 12. The method makes it possible to find the energies and wave functions of bound states and relatively narrow quasibound states in such a potential. We took all such states into account in calculating the structures of both the one-phonon states and the partial transition densities (6) and (7).

The parameters of the Woods-Saxon potential and the values of the pairing-interaction constants corresponding to the single-particle basis are given in Refs. 13 and 14.

The coefficients $\psi^{\lambda i}_{jj'}$ and $\varphi^{\lambda i}_{jj'}$ occurring in the definition of the one-phonon wave function (4) were calculated with the aid of the RPAS program,[15] using known formulas of the RPA with separable effective forces.[8] The one-phonon $M\lambda$ states were generated by effective separable spin-multipole forces of the form

$$V^{\lambda}_{\sigma\lambda-1}(\mathbf{r}_1,\mathbf{r}_2) = 1/2(\varkappa_0^{(\lambda-1,\lambda)} + \varkappa_1^{(\lambda-1,\lambda)}\tau_1\tau_2)r_1^{\lambda-1}r_2^{\lambda-1}$$
$$\times\sum_{\mu'}[\sigma_1Y_{\lambda\mu}(\Omega_1)]_{\lambda\mu'}[\sigma_2Y_{\lambda\mu}(\Omega_2)]_{\lambda-\mu'}. \quad (8)$$

The isoscalar and isovector constants $\varkappa_0^{(\lambda-1,\lambda)}$ and $\varkappa_1^{(\lambda-1,\lambda)}$ of the effective interaction $V^{\lambda}_{\sigma\lambda-1}(\mathbf{r}_1,\mathbf{r}_2)$ are the model parameters. The position of the $M\lambda$ resonance and the structure of the one-phonon states constituting it depend to a considerable extent on these parameters. In our approach, the choice of these constants can be based only on the available experimental data and very simple qualitative estimates. However, an indefinite situation has recently arisen as regards the existence of $M1$ resonances in medium-mass and heavy nuclei,[4,5] and this makes it difficult to choose the force parameters, at least for $M1$ excitations. Nevertheless, in the present work we shall use the values of $\varkappa_0^{(\lambda-1,\lambda)}$ and $\varkappa_1^{(\lambda-1,\lambda)}$ given earlier in Refs. 13 and 14 because they reproduce quite satisfactorily the experimental data[16] on 1^+ and 2^- states in ^{58}Ni, the data[17] on $M1$ radiative strength functions for nuclei with $A \sim 140$, concerning which no doubts have yet arisen, and the results of Richter *et al.*[5] on the $M2$ resonance. These values of the constants agree (at least in order of magnitude) with the estimates of Ref. 18.

The present calculations were accordingly carried through using the following values of the constants:

$$\varkappa_0^{(\lambda-1,\lambda)} = 0, \quad \varkappa_1^{(\lambda-1,\lambda)} = -\frac{4\pi\cdot 28}{A\langle r^{2\lambda-2}\rangle}\ \frac{\text{MeV}}{\text{F}^{2\lambda-2}}. \quad (9)$$

We used the following values[13,14] for the effective gyromagnetic factors: $g_s^* = 0.8\,g_s^{free}$ and $g_l^* = g_l^{free}$. It should be borne in mind that RPA calculations using these parameter values unambiguously indicate the existence of the $M1$ resonance. This question will also be touched upon in Sections 4 and 5.

3. CURRENT TRANSITION DENSITIES FOR ONE-PHONON 2^- STATES

As was noted above, the structure of the anomalous-parity excited states affects the electron inelastic-scattering cross section through the current transition densities defined by formulas (6) and (7). The wave functions for the one-phonon 1^+ and 2^- resonance states differ substantially from one another. No more than two or three two-quasiparticle components (corresponding to spin-orbit doublets) contribute to the structure of the 1^+ states, and frequently one of them dominates the others. The 2^- states have a collective structure, i.e., their wave functions are superpositions of many two-quasiparticle components.[14,19]

The CTD of a few of the 1^+ and 2^- resonance states are shown in Fig. 1. The CTD of magnetic dipole states are evidently of surface type, while those of magnetic quadrupole states are of volume type.[20] It is interesting that the charge transition densities of the

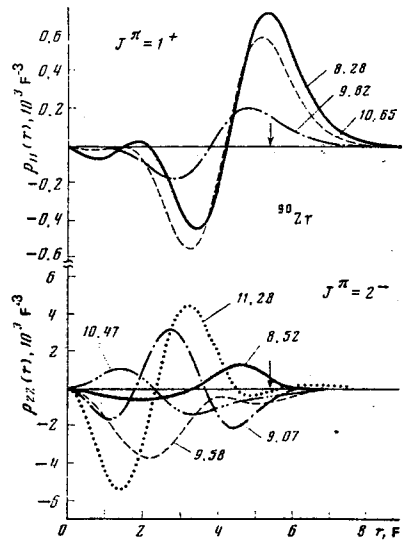

FIG. 1. Current transition densities of anomalous-parity one-phonon states in ^{90}Zr. The numbers give the excitation energies of the states in MeV. The arrow marks the radius R_0 of the nucleus.

collective 1^- states that form the giant dipole resonance, as calculated with separable dipole forces, i.e. with forces having the same radial dependence as the forces (8) for $\lambda = 2$, are quite evidently of surface type.[9]

The main contribution to the CTD of one-phonon $M1$ excitations comes from the magnetic component $\rho^m_{\lambda\lambda}(r)$, in which the term $\sim d/dr$ plays the principal part. The contribution from the convection current to the CTD of $M2$ excitations is larger; here $\rho^c_{\lambda\lambda}(r)$ amounts to 30–50%. However, the contribution from terms $\sim d/dr$ remains important, as before.

The structure of the collective one-phonon 2^- states is sensitive to the strength parameters of the effective forces. The CTD's plotted in Fig. 1 were calculated for the values of $\varkappa_0^{(\lambda-1,\lambda)}$ and $\varkappa_1^{(\lambda-1,\lambda)}$ given by (9). How the CTD's vary as the constants $\varkappa_0^{(\lambda-1,\lambda)}$ and $\varkappa_1^{(\lambda-1,\lambda)}$ are changed can be seen from Fig. 2. In order to be able to compare the changes in the CTD with the changes in the structure and other characteristics of the states, we have listed the appropriate data in Table I. On comparing Fig. 2 with the data in Table I,

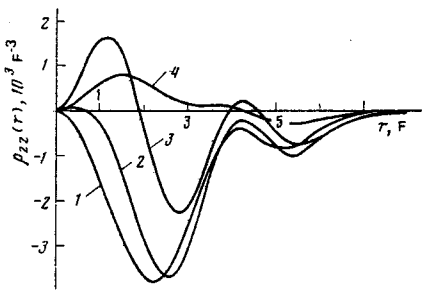

FIG. 2. Current transition densities for the one-phonon 2^- state of ^{90}Zr at $E_x = 9.58$ MeV as calculated for the following values of the isovector spin-dipole interaction constant [$\varkappa_1^{(12)}$ denotes the value of this constant calculated from formula (9)]. Curves: 1—$\varkappa_1^{(12)}$, 2—$0.5\varkappa_1^{(12)}$, 3—$0.2\varkappa_1^{(12)}$, 4—$0.1\varkappa_1^{(12)}$. Also see Table I.

TABLE I. Energies, $B(M2)$ values, and differential cross sections $d\sigma/d\Omega$ (at two incident-electron energies E_0 and $\theta = 165°$) of collective 2^- states of ^{90}Zr for several values of the isovector spin-dipole interaction constant.

	$\varkappa_1^{(12)}$	$0.5\varkappa_1^{(12)}$	$0.2\varkappa_1^{(12)}$	$0.1\varkappa_1^{(12)}$
E_x, MeV	9.58	9.48	9.33	9.31
$B(M2)$, μ_N^2 F^2	710	1260	810	720
$\frac{d\sigma}{d\Omega}\cdot\frac{\Phi M^2}{cp}$ $E_0=50$ MeV	$0.46\cdot10^{-5}$	$0.67\cdot10^{-5}$	$0.33\cdot10^{-5}$	$0.22\cdot10^{-6}$
$\frac{d\sigma}{d\Omega}\cdot\frac{\Phi M^2}{cp}$ $E_0=100$ MeV	$0.43\cdot10^{-6}$	$0.32\cdot10^{-6}$	$0.25\cdot10^{-7}$	$0.18\cdot10^{-7}$
Structure of the state				
$(2p_{3/2}-3s_{1/2})_n$	29.7%	13.8%	1.4%	<1%
$(1f_{5/2}-1g_{7/2})_n$	11.5%	6.0%	<1%	<1%
$(1g_{9/2}-1h_{11/2})_n$	5.0%	4.8%	1%	<1%
$(2p_{1/2}-2d_{3/2})_n$	2.7%	5.4%	13.5%	1.4%
$(2p_{3/2}-2d_{3/2})_z$	26.5%	41.1%	27.4%	1.5%
$(1f_{7/2}-1g_{9/2})_z$	14.6%	17.1%	5.3%	<1%
$(1f_{5/2}-2d_{5/2})_z$	2.4%	5.3%	50.0%	96.7%

Note. $\varkappa_1^{(12)}$ represents the value calculated with Eq. (9). The variations of the CTD may be compared with the variations in the structures of the states.

it will be seen that when the constant $|\varkappa_1^{(12)}|$ changes by a factor of two, the collective character of the 2^- state and the qualitative trend of the CTD remain relatively unchanged. More substantial changes in the CTD take place when the 2^- state becomes noncollective and the CTD is determined by contributions from two or three two-quasiparticle components. It is also significant that such integral characteristics of the individual 2^- states as the excitation energy E_x and the $B(M2)$ value are much less sensitive than the CTD to changes in $\varkappa_1^{(12)}$. For example, when $\varkappa_1$ changes by a factor of 10, $B(M2)$ changes by a factor of 1.5–2.0. This can be understood, in part, since $B(M2)$ is nothing but the integral of $\rho_{22}(r)$. A more delicate characteristic of the state will be the cross section for its excitation in e, e' scattering, especially at high momentum transfers. The values of $d\sigma/d\Omega$ at $\theta = 165°$ are also listed in the Table for two values of the incident-electron energy E_0. For relatively small momentum transfers q, a decrease in $|\varkappa^{(12)}|$ first causes no appreciable changes in $d\sigma/d\Omega$, the cross section beginning to decrease appreciably only when the states become essentially noncollective. At large momentum transfers, $d\sigma/d\Omega$ becomes sensitive to the fine details of the CTD and may depend very strongly on $|\varkappa_1^{(12)}|$, increasing as $|\varkappa^{(12)}|$ decreases.

4. DEPENDENCE ON THE MOMENTUM TRANSFER AND TARGET-NUCLEUS MASS NUMBER OF THE PROBABILITY FOR EXCITATION OF ONE-PHONON 1^+ AND 2^- STATES IN ELECTRON INELASTIC SCATTERING

Now let us turn to the discussion of the results of strict calculations of the cross sections for excitation of 1^+ and 2^- states in e, e' scattering. We emphasize once more that we calculated the structures of the excited states in the random phase approximation. This imposes certain limitations on the possibility of comparing the calculated results with the experimental data. Thus, in ^{90}Zr, ^{140}Ce, and ^{208}Pb, the interaction with two-phonon configurations has little effect on the $M1$ and $M2$ resonances,[13,14] and RPA calculations reproduce the experimental data quite satisfactorily. For ^{58}Ni the situation is different; here the experi-

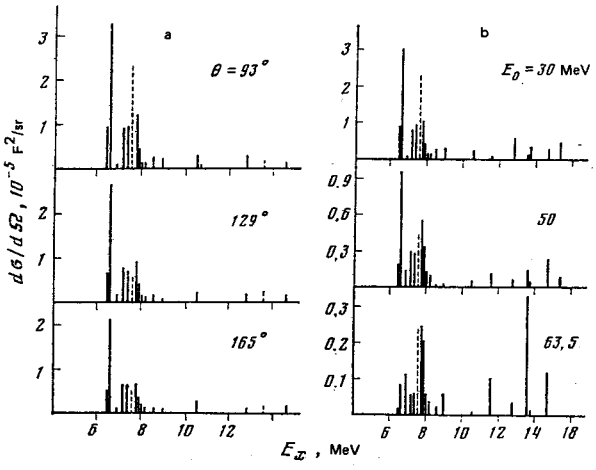

FIG. 3. Differential cross sections for electroexcitation of one-phonon states of ^{208}Pb with $J^\pi = 1^+$ (dashed lines) and $J^\pi = 2^-$ (full lines) for the incident-electron energy $E_0 = 40$ MeV and several scattering angles θ (plots a) and for the scattering angle $\theta = 165°$ and several incident-electron energies E_0 (plots b).

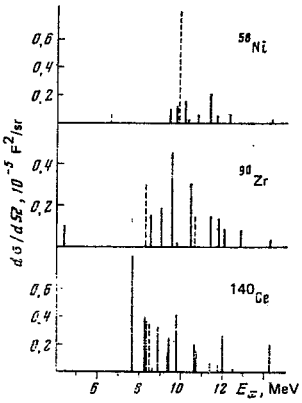

FIG. 4. Differential cross sections for excitation by electron inelastic scattering of one-phonon 1^+ (dashed lines) and 2^- (full lines) states in the spherical nuclei ^{58}Ni, ^{90}Zr, and ^{140}Ce: incident electron energy $E_0 = 40$ MeV, scattering angle $\theta = 156°$.

mental results of Lindgren *et al.*[16] can be explained only by invoking the effect of that interaction. There are accordingly some limitations on the comparison of our calculations with the experimental data.

By altering the incident-electron energy or the scattering angle, one can vary the momentum transferred by the electron to the nucleus. Because of the different forms of the CTD, different nuclear levels will be excited with different probabilities when the momentum transfer q is the same and, what is also very important, when q varies the relative probabilities for excitation of the various levels will also vary. Thus, it is possible, at least in principle, to choose the experimental conditions so that states of a certain type will be preferentially excited.

This general assertion is demonstrated in Fig. 3, which shows differential cross sections for electron inelastic scattering from ^{208}Pb with excitation of one-phonon 1^+ and 2^- states having excitation energies E_x in the range 0–15 MeV. The changes in q in Fig. 3a are due to changes in the scattering angle θ, and those in Fig. 3b are due to changes in the incident-electron energy. When q is small, so that the long-wave approximation is valid, the ratios of the differential cross sections $d\sigma/d\Omega$ for excitation of different states with given J^π values are virtually the same as the corresponding ratios of the $B(MJ)$ values. As q increases, the relative contributions of individual states to the total cross section begin to change. The maximum of the Bessel function $j_\lambda(qr)$, whose convolution with $\rho_{\lambda\lambda}(r)$ occurs in the formula for the e, e'-scattering cross section, shifts into the interior of the nucleus as q increases; increasing q will therefore lead to high probabilities for excitation of states whose CTD are of volume type. That is precisely why the contribution to the cross section from 1^+ states decreases: those states get further and further lost in the background of the 2^- excitations. The relative probabilities for excitation of different 2^- states also vary. This is seen most clearly in the case of the two 2^- states with excitation energies E_x of 6.6 and 13.6 MeV. The first of these states has the maximum $B(M2)$ value and is strongly excited when q is rather small. The second of these states, on the other hand, has a fairly small $B(M2)$ value, but then it is strongly excited when $q > 1$ F^{-1} (see Fig. 3b below). In general, as q increases the probability for excitation of 2^- states with $6 < E_x < 9$ MeV, which exhaust a considerable fraction of the total $B(M2)$ value, falls rapidly, while the cross sections for excitation of states with $11 < E_x < 15$ MeV, whose contribution to the total $B(M2)$ value is small, either remain constant or even increase. As a result, one can distinguish two regions in the spectrum of ^{208}Pb below $E_x = 15$ MeV in which the probability for excitation of 2^- states is enhanced when $q > 1$ F^{-1}. This example shows once more that the theoretical results must be compared with directly measured quantities, or else the experimental data must be processes [e.g., to extract the $B(M2)$ values from the e, e'-scattering cross sections], using sufficiently consistent theoretical models.

Figure 4 shows how the probabilities for excitation of resonance one-phonon 1^+ and 2^- states of spherical nuclei vary with increasing mass number A. As A increases, first, the spectrum becomes enriched in one-phonon 2^- states and the probabilities for excitation of individual 2^- states increase; second, the probabilities for excitation of the rather few one-phonon 1^+ states decrease. Thus, as A increases it becomes more and more difficult to distinguish the contribution to the cross section from magnetic dipole excitations against the background of magnetic quadrupole ones. We must say that this fact also follows from simple qualitative estimates in the long-wave approximation. Actually, when q is small we have $(d\sigma/d\Omega)_{M\lambda} \sim q^{2\lambda} B(M\lambda)$. If we use Weisskopf's estimates[21] for the $B(M\lambda)$, we obtain[1)] for the ratio of the cross sections for excitation of $M2$ and $M1$ states.

$$\left(\frac{d\sigma}{d\Omega}\right)_{M2} \Big/ \left(\frac{d\sigma}{d\Omega}\right)_{M1} \sim q^2 A^{2/3}. \qquad (10)$$

This A-dependence of $d\sigma/d\Omega$ is perhaps one of the rea-

sons (which we pointed out earlier[22]) why searches for $M1$ resonances in heavy nuclei have been unsuccessful.

5. FORM FACTORS FOR ONE-PHONON STATES

The spins and parities of states excited in e, e' scattering are frequently determined by comparing the experimental form factors, i.e., the quantities $(d\sigma/d\Omega)/(d\sigma/d\Omega)_{\text{Mott}}$ regarded as functions of the momentum transfer q, with the form factors calculated using some nuclear model or other. The form factors for different nuclear excitations differ quite appreciably from one another, and that is what makes it possible to determine the quantum numbers of excited states.

Let us examine the behavior of the form factors of the one-phonon 1^+ and 2^- states in ^{140}Ce for which the experimental form factors are known. The form factors for individual one-phonon 2^- states of ^{140}Ce in the excitation-energy region $7.5 < E_x < 10$ MeV are plotted in Fig. 5. When q is small and the long-wave approximation is valid, the form factors for different states are close together in magnitude and behave virtually alike as functions of E_0 (or of q, since θ is constant). Some differences begin to arise when $E_0 \gtrsim 30$ MeV, and when $E_0 > 80$ MeV the form factors for the individual states behave quite differently; here the individual form of the CTD for each state manifests itself in full measure. The behavior of the form factor of the state at $E_x = 9.81$ MeV is noteworthy. The 9.81-MeV state apparently manifests itself in e, e' scattering in the same way as the 6.6-MeV state of ^{208}Pb, which was discussed in Section 4. This state has a considerable $B(M2)$ value as well as a considerable probability for excitation when q is small, but the form of its CTD is such that it is excited only weakly when q is large. It is interesting that, despite the rather sharp variations of the form factors for individual 2^- states, the sum of the form factors for all the states in the E_x interval being examined is a fairly smooth function of E_0. The sum of the form factors is in quite satisfactory agreement with the experimental data,[5] as is evident from Fig. 6. The experimental data on the form factors were obtained for two values of the scattering angle θ: 165° and 93°. The agreement is quite

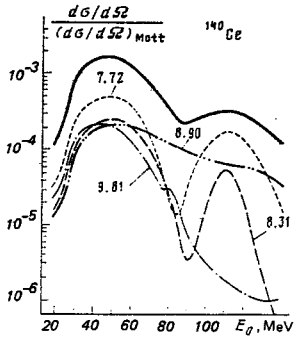

FIG. 5. Form factors for one-phonon 2^- states of ^{140}Ce in the excitation-energy range $7.5 < E_x < 10$ MeV (scattering angle $\theta = 165°$). The numbers give the energies of the states in MeV. The full curve represents the sum of all the form factors shown.

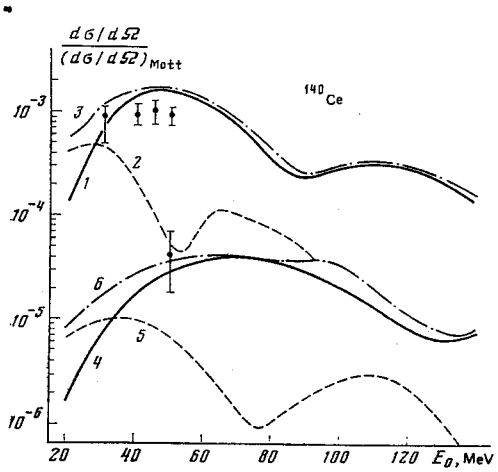

FIG. 6. Sums of the form factors for one-phonon states with $J^\pi = 1^+$ (dashed curves) and $J^\pi = 2^-$ (full curves) of ^{140}Ce in the interval $7.5 < E_x < 10$ MeV and sums of the $M1$ and $M2$ form factors (dash-dot curves) for the scattering angles $\theta = 165°$ (curves 1, 2, and 3) and $\theta = 93°$ (curves 4, 5, and 6). The experimental points were taken from Ref. 5.

satisfactory, both in absolute value (we emphasize that the theoretical form factors were not normalized in any special way) and in the behavior of the form factor as a function of E_0, and this permits one to conclude that it was precisely 2^- states that were excited in the experiment. The authors of Ref. 5 themselves reached a similar conclusion from a comparison of their experimental data with calculations based on the MSI model.[23] As was pointed out in Ref. 24, however, these experimental data[5] do not rule out the presence of 1^+ states with $B(M1) \simeq 10\mu_N^2$ in the investigated E_x interval. The corresponding form factors are also presented in Fig. 6. The total form factor for the 1^+ and 2^- states does not decrease so rapidly with E_0 as the $M2$ form factor alone, and this agrees better with the trend of the experimental points for $\theta = 165°$. It is evident from Fig. 6, as well as from the results presented in Section 4, that in order reliably to distinguish the 1^+ excitations against the background of 2^- ones it is necessary to have measurements at lower incident-electron energies than were used in Ref. 5. Of course, as our calculations show, the contribution from the $M1$ resonance at $\theta = 93°$ is appreciable at higher energies ($E_0 \simeq 100$ MeV) in the vicinity of the second maximum of the $M1$ form factor. It is not ruled out, however, that magnetic states with $\lambda > 2$ will be excited with high probability at these energies, and this presents additional difficulties in distinguishing the 1^+ states.

6. CONCLUSION

There are two basic points to be distinguished in the present work. First, the current transition densities of anomalous-parity states have been calculated within the limitations of the quasiparticle-phonon nuclear model. It turned out that the CTD of one-phonon 1^+ states are of surface type, and those of the one-phonon 2^- states are of volume type. The dependence of the CTD of collective 2^- states on the force parameters of

the model have been investigated. Our calculated CTD values can be used to describe the inelastic scattering of elementary particles (electrons, protons, pions) from nuclei. Second, we have examined how electron inelastic scattering with excitation of anomalous-parity states is described with the CTD of the quasiparticle-phonon model. The model reproduces the available experimental data on the excitation of 2^- states in ^{140}Ce satisfactorily. Moreover, our calculations indicate that the lack of success in searching for $M1$ resonance in heavy nuclei may be associated with the difficulty of distinguishing 1^+ excitations against the background of 2^- ones at the incident-electron energies and scattering angles used in Ref. 5.

The authors thank Professor V. G. Solov'ev for his interest in the work, and Ch. Stoyanov and V. V. Voronov for discussing problems touched upon in the present work and for remarks made while reading the manuscript.

[1)]It is also evident from Eq. (10) that the cross section for excitation of $M2$ states will rise more rapidly with increasing q than the cross section for excitation of $M1$ states (see the beginning of the present Section).

[1]R. Pitthan and Th. Walcher, Phys. Lett. 36B, 563 (1971); Z. Naturforsch. 27A, 1683 (1972).
[2]S. Fukuda and Y. Torizuka, Phys. Rev. Lett. 29, 1109 (1972).
[3]R. A. Lindgren *et al.*, Phys. Rev. Lett. 35, 1423 (1975).
[4]A. Richter, Proc. Sendai Conf. on Electro- and Photoexcitations (Suppl. Research Rept., Lab. Nucl. Sci.) V. 10, Tohoku Univ., Tomizawa, Sendai, Japan, 1977, p. 195.
[5]A. Richter, Proc. Intern. Conf. on Nucl. Phys. with Electromagnetic Interactions (Arenhövl and Dreschel, editors), Mainz, 1979, p. 19.
[6]N. G. Goncharova *et al.*, Yad. Fiz. 27, 1183 (1978) [Sov. J. Ncul. Phys. 27, 627 (1978)]; Izv. Akad. Nauk SSSR, Ser. Fiz. 44, 168 (1980) [Bull. Acad. Sci. USSR, Phys. Ser.].
[7]J. Speth and J. Wambach, Nucl. Phys. A347, 389 (1980).
[8]V. G. Solove'ev, Teoriya slozhnykh yader (Theory of complex nuclei) Nauka, Moscow, 1971 (Eng. Transl., Pergamon Press, N.Y., 1976); Fiz. Elem. Chastits At. Yadra 9, 860 (1978) [Sov. J. Part. Nucl. 9, 343 (1978)].
[9]S. V. Akulinichev *et al.*, Yad. Fiz. 28, 883 (1978) [Sov. J. Nucl. Phys. 28, 453 (1978)]; S. V. Akulinichev and V. M. Shilov, Yad. Fiz. 27, 670 (1978) [Sov. J. Nucl. Phys. 27, 358 (1978)].
[10]S. T. Tuan, L. E. Wright, and D. S. Onley, Nucl. Instr. Meth. 60, 70 (1968).
[11]H. C. Lee, Chalk River Nucl. Lab. Preprint AECL-39, Chalk River, Ontario, 1975.
[12]J. Bang *et al.*, Nucl. Phys. A261, 59 (1976). M. Kh. Gizzatkulov *et al.*, JINR, R11-10029, Dubna, 1976.
[13]V. Yu. Ponomarev *et al.*, Nucl. Phys. A323, 446 (1979).
[14]A. I. Vdovin *et al.*, Yad. Fiz. 30, 923 (1979) [Sov. J. Nucl. Phys. 30, 479 (1979)].
[15]Ch. Stoyanov and I. P. Yudin, JINR Communication R4-11076, Dubna, 1977.
[16]R. A. Lindgren *et al.*, Phys. Rev. C 14, 1789 (1976).
[17]R. E. Chrien *et al.*, Phys. Rev. C 9, 1622 (1974); R. J. Holt and H. E. Jackson, Phys. Rev. C 12, 56 (1975); R. M. Laszewski, R. J. Holt, and H. E. Jackson, Phys. Rev. C 13, 2257 (1976).
[18]B. Castel and I. Hamamoto, Phys. Lett. 65B, 27 (1926).
[19]A. I. Vdovin *et al.*, Tez. Dokl. XXX soveshch. po yadernoĭ spektroskopiĭ i strukture atomnogo yadra (Abstracts of the thirtieth conf. on nuclear spectroscopy and nuclear structure), Leningrad, Nauka 1980, p. 166.
[20]A. I. Vdovin *et al.*, JINR Communication R4-11081, Dubna, 1977. V. Yu. Ponomarev and A. I. Vdovin, JINR Communication R4-80-392, Dubna, 1980.
[21]J. M. Blatt and V. F. Weisskopf, Theoretical nuclear physics, Wiley, N.Y., 1952.
[22]V. Yu. Ponomarev *et al.*, Abstracts of the Intern. Symp. on highly excited states in nuclear reactions, Osaka, 1980, p. 23.
[23]W. Knüpfer and M. G. Huber, Phys. Rev. C 14, 2254 (1976).
[24]V. Yu. Ponomarev *et al.*, Phys. Lett. 97B, 4 (1980).

Translated by E. Brunner